

Concentration Fluctuations in Ethanol/Dodecane Mixtures. A Light-Scattering and Ultrasonic Spectroscopy Study

U. Dürr, S. Z. Mirzaev,[†] and U. Kaatz*^{*}

Drittes Physikalisches Institut, Georg-August-Universität, Bürgerstrasse 42–44, D-37073, Germany

Received: January 20, 2000; In Final Form: July 19, 2000

Dynamic light-scattering measurements of liquid ethanol/dodecane mixtures have been performed using a self-beating digital photon correlation spectrometer. The binary system exhibits an upper critical consolute point at a mole fraction $x_c = 0.687$ of ethanol. The critical temperature of our sample was $T_c = 285.64 \pm 0.05$ K. Along with shear viscosity data the decay rate of the autocorrelation function of the scattered light has been used to determine the mutual diffusion coefficient D , the fluctuation correlation length ξ , and the characteristic relaxation rate ω_D of the order parameter fluctuations as a function of reduced temperature. For the mixture of critical composition these quantities follow power law behavior, as predicted theoretically. The amplitude of the relaxation rate of the ethanol/dodecane system is $\omega_0 = (8.0 \pm 0.2) \times 10^9 \text{ s}^{-1}$ from dynamic light scattering, which compares with $\omega_0 = 2.8 \times 10^9 \text{ s}^{-1}$ and $\omega_0 = 4.4 \times 10^9 \text{ s}^{-1}$ as resulting from broadband ultrasonic spectra. Fitting the light-scattering data at different scattering angles to the universal dynamic (Kawasaki) function yields $\omega_0 = (7.7 \pm 0.7) \times 10^9 \text{ s}^{-1}$. Critical mixtures with an amount of 0.2% (w/w) water added resulted in an enhancement of T_c by about 3.5 K and in a small increase (10%) in the amplitude D_0 of the mutual diffusion coefficient. Light-scattering data for five ethanol/dodecane mixtures of noncritical composition are in conformity with the pseudospinodal conception. It remains unclear, however, whether noncritical exponents have to be used in the power laws. Using the critical exponents in the evaluation of data the amplitude ξ_0 of the correlation length displays a relative maximum at the critical composition where D_0 adopts a relative minimum.

Introduction

Many properties of binary liquid mixtures exhibit striking anomalies as a critical demixing point is approached. At the critical point the mutual diffusion coefficient D vanishes, combined with the occurrence of large local fluctuations in concentration that decay very slowly and reach effectively macroscopic scale. This behavior is reflected by a power law divergence of the correlation length

$$\xi(T) = \xi_0 t^{-\nu} \quad (1)$$

Here $t = |T - T_c|/T_c$ is the reduced temperature, T_c is the critical temperature, and ξ_0 and ν are the amplitude and critical exponent of the correlation length ξ . Connected with those concentration fluctuations are corresponding fluctuations in the compressibility, density, and optical index of refraction. The result is a remarkable increase in the turbidity, known as critical opalescence.¹ Because the coupling of sonic fields to the compressibility and energy fluctuations, an acoustical anomaly is also observed: when a critical demixing point is approached, the sonic attenuation coefficient increases considerably. The sound attenuation in excess of the classical attenuation^{2,3} is not a scattering process,^{4,5} similar to critical opalescence, but has been ascribed to the coupling between the long-range density fluctuations and the variations in the temperature and density induced by the acoustical field.⁶ Dynamic light scattering and ultrasonic spectrometry thus are complementary methods in the

investigation of critical demixing phenomena, gaining valuable insights into the dynamical characteristics of the phase transition and allowing quantities such as the correlation length (eq 1) and the relaxation rate

$$\omega_D = 2D/\xi^2 \quad (2)$$

of the order parameter fluctuations to be investigated.

Basically, three different categories of theoretical approaches have been proposed to describe the acoustical anomaly near critical points: the mode coupling theory,^{6–17} the Bhattacharjee–Ferrell theory^{18–20} based on the dynamic scaling hypothesis,^{21,22} and the renormalization group theory.^{23–30}

Ultrasonic spectra have been measured for several binary mixtures and have been compared with theoretical scaling functions.^{31–46} For nonassociating liquids the theoretical predictions are good but often do not exactly describe the measured ultrasonic attenuation. For this reason, much interest is directed toward crossover corrections for scaling, enabling the theoretical approaches to be more adequately used apart from the critical point where large noncritical contributions to the sonic spectrum may exist.^{47, 48}

For associating liquids our knowledge of the critical attenuation is still insufficient. An example is the $[\alpha_\lambda^c(f,T) - \alpha_\lambda^b(f,T)]/\alpha_\lambda^c(f,T_c)$ versus Ω plot for the methanol/cyclohexane mixture of critical composition given in Figure 1. The data measured at different frequencies f neither fall on the same curve nor are the experimental data adequately represented by the theoretical scaling function $F_{\text{BF}}(\Omega)$ defined below (eqs 7, 8). Here $\alpha_\lambda^c(f,T)$ denotes the ultrasonic attenuation per wavelength

* Author for correspondence.

[†] Permanent address: Heat Physics Department, Uzbek Academy of Sciences, Katartal 28, Tashkent, 700135 Uzbekistan.

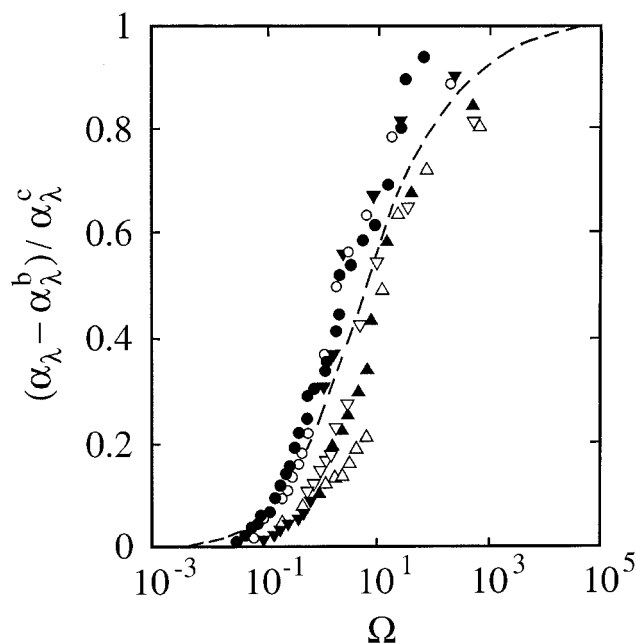


Figure 1. Normalized sonic attenuation coefficient per wavelength, excluding the background contribution, for the system methanol/cyclohexane⁴⁰ displayed as a function of reduced frequency Ω . Figure symbols indicate the frequency of measurement: ●, 5 MHz; ○, 7 MHz; ▼, 10 MHz; ▽, 15 MHz; ▲, 21 MHz; △, 30 MHz. The dashed curve is the graph of the Bhattacharjee–Ferrell scaling function eq 8 with the amplitude of the characteristic relaxation rate adjusted to $\omega_0 = 1.6 \times 10^{12} \text{ s}^{-1}$ to fit the data ($\omega_0 = 3.5 \times 10^{10} \text{ s}^{-1}$ follows from the amplitudes of the viscosity and the fluctuation correlation length⁴⁰ if eq 5 is used).

of the mixtures of critical composition at the frequency f and at the temperature T , $\alpha_\lambda^b(f, T)$ is the noncritical background contribution to the total attenuation, and $\alpha_\lambda^c(f, T_c)$ is the critical attenuation per wavelength at the critical temperature T_c . In the reduced frequency

$$\Omega = 2\pi f / \omega_D \quad (3)$$

the relaxation rate

$$\omega_D = \omega_0 t^{-z\nu} \quad (4)$$

of the order parameter fluctuations is used for normalization, whereas z and ν are critical exponents. If noncritical background contributions to η can be neglected, the amplitude

$$\omega_0 = k_B T / (3\pi\eta_0\xi_0^3) \quad (5)$$

is related to the shear viscosity amplitude η_0 , defined by

$$\eta(T) = \eta_0 t^{-(z-3)\nu} \quad (6)$$

k_B is Boltzmann's constant. In Figure 1 the Bhattacharjee–Ferrell scaling function

$$F_{\text{BF}}(\Omega) = \alpha_\lambda^c(f, T) / \alpha_\lambda^c(f, T_c) \quad (7)$$

has the form²⁰

$$F_{\text{BF}}(\Omega) = [1 + 0.414(\Omega_{1/2}/\Omega)^{1/2}]^{-2} \quad (8)$$

where the best theoretical value for the dimensionless half-attenuation frequency is $\Omega_{1/2} = 2.1$.

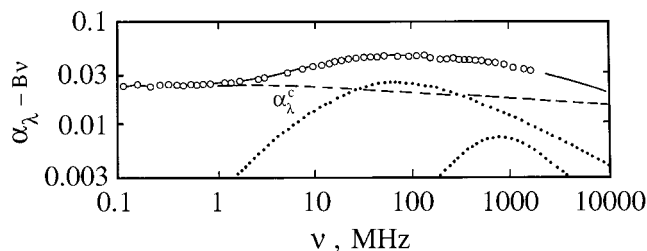


Figure 2. Ultrasonic excess attenuation spectrum for an isobutoxy-ethanol/water mixture of critical composition at 26.3 °C ($t = 2 \times 10^{-4}$). The dashed curve shows the Bhattacharjee–Ferrell spectrum α_λ^c of the critical contribution. Dotted curves indicate further contributions with relaxation characteristics to the total spectrum.⁷⁹

The discrepancy between the experimental findings and the theoretical predictions in Figure 1 may only in part reflect a nonperfect scaling function. Broadband ultrasonic attenuation measurements of binary mixtures of associating liquids reveal α_λ spectra which, besides a critical part and a background contribution proportional to f , contain additional contributions with relaxation characteristics (Figure 2). Frequently it is not clear how far the relaxation contributions are due to particular chemical equilibria within the liquid and to what extent these contributions may just compensate imperfections of the theoretical models of critical concentration fluctuations. We therefore decided to perform a comparative acoustic relaxation and light-scattering study of the rather simple ethanol/dodecane system. We reconsider our previous results from broadband ultrasonic spectrometry⁴⁹ yielding the relaxation rate ω_D as a function of temperature from the analytical description of the experimental relaxation spectra. These ω_D data are compared with those obtained from shear viscosities and from the diffusion coefficient derived from dynamic light-scattering measurement. The suggestive relation^{9,50}

$$D = k_B T / (6\pi\eta\xi) \quad (9)$$

is used for this purpose. Equation 9 may be taken as an analogous application of the Einstein–Stokes relation for the diffusion of a spherically shaped Brownian particle of radius ξ . Along with eq 2 this relation yields

$$\omega_D = k_B T / (3\pi\eta\xi^3) \quad (10)$$

In addition to the study of the mixture of critical composition, dynamic light-scattering data for noncritical concentrations were taken and are treated in terms of the pseudospinodal conception introduced by Chu et al.⁵¹ Also considered are effects of impurities upon the critical temperature, mutual diffusion coefficient, and correlation length. Light-scattering measurements on ethanol/dodecane mixtures of critical composition, with small amounts of water added, have been performed for this purpose.

Experimental Section

Ethanol/Dodecane Mixtures. Ethanol (99.8%) and *n*-dodecane (99%) were used as supplied by the manufacturer (Merck, Darmstadt, Germany). Samples were prepared by weighing appropriate amounts of the constituents into suitable flasks. The critical parameters and also the demixing temperature of the noncritical mixtures have been obtained from monitoring the appearance of the meniscus when slowly cooling the sample. We found a critical temperature $T_c = 285.64 \pm 0.05 \text{ K}$ for the critical mixture with mole fraction $x_c = 0.687$ of ethanol. T_c is

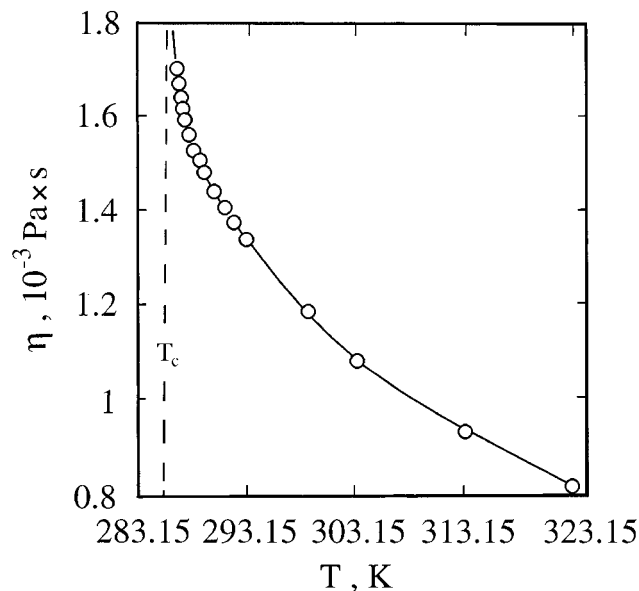


Figure 3. Shear viscosity η of the ethanol/dodecane mixture of critical composition as a function of temperature. The curve is drawn just to guide the eye.

in fair agreement with literature data (284.6 K,⁵² 285.0 K,⁵³ 286.71 K⁵⁴), and is about 1 K smaller than in our previous acoustical relaxation study (286.7 \pm 0.05 K).⁴⁹

Shear Viscosities. For use in eq 10 the (static) shear viscosity of the ethanol/dodecane mixture of critical composition has been measured in a temperature range up to 40 K above T_c . A falling ball viscometer (Haake, Berlin, Germany) has been used for this purpose. The temperature of the viscometer was controlled to within 0.02 K by circulating thermostat fluid. In Figure 3 the η values are displayed as a function of temperature. Close to T_c ($0 \leq t \leq 2 \times 10^{-2}$) the viscosity data follow a power law behavior as predicted by eq 6, with a fitted critical amplitude $\eta_0 = 1.26 \pm 0.01$ mPa s and the fixed critical exponent $(z - 3)\nu = 0.0378$.^{9,55,56} We found an amplitude $\eta_0 = 1.21 \pm 0.02$ mPa s if the more recent accurate value⁵⁷ of the viscosity exponent $(z - 3)\nu = (0.0690 + 0.0006)\nu = 0.0435 \pm 0.0004$ is used for the data at $0 \leq t \leq 2 \times 10^{-2}$. Because of the temperature dependence of the background viscosity and because of the crossover from critical to noncritical behavior the power law (eq 6) holds close to the critical point only. Hence if all measured η data are considered, a somewhat reduced viscosity amplitude follows [$\eta_0 = 1.08 \pm 0.05$ mPa s if $(z - 3)\nu = 0.0435$ and $0 \leq t \leq 0.14$].

Acoustical Attenuation Spectrometry. At altogether 13 temperatures the ultrasonic attenuation coefficient of the mixture of critical composition had been measured as a function of frequency f .⁴⁹ To monitor critical slowing in the critical contribution α^c to the attenuation coefficient, particular attention had been paid to the lower part ($100 \text{ kHz} \leq f \leq 2 \text{ MHz}$) of the measuring frequency range.⁴⁹ A planoconcave cavity resonator method was used at those frequencies.⁵⁸ To also account appropriately for the asymptotic high-frequency background part in α , some spectra had been measured up to 500 MHz. A biplanar cavity resonator cell had been used for this purpose ($1 \text{ MHz} \leq f \leq 15 \text{ MHz}$)⁵⁹ and a pulse-modulated wave transmission technique at variable sample thickness had been also applied ($15 \text{ MHz} \leq f \leq 500 \text{ MHz}$).⁶⁰

Dynamic Light Scattering. We used a self-beating digital photon correlation spectrometer^{61–64} to measure the decay rate Γ of the time autocorrelation function of the light quasielastically scattered from the sample. In the hydrodynamic limit the decay

rate Γ_q at a given wave vector obeys the equation

$$\Gamma_q = Dq^2 \quad (11)$$

relating it to the mutual diffusion coefficient D and the amount

$$q = 4\pi n \lambda_0^{-1} \sin(\theta/2) \quad (12)$$

of the wave vector selected by the scattering geometry. Here n is the index of refraction of the sample, λ_0 is the wavelength of the incident light, and θ is the scattering angle.

To utilize the θ dependence in the decay rate, the cylindrically shaped specimen cell was precisely placed on a goniometer system. Measurements have always been performed at 24 scattering angles between 30° and 145° to ensure that the setup was adequately adjusted and that the spectra were not affected by multiple reflections and isotropy effects. The cell (sample volume 2 mL) was provided with a special planar window for an effective reduction of diffraction of the incident and the unscattered light. The temperature of the sample was controlled to within 0.02 K by thermostat fluid that was circulated through two chambers positioned below and above the scattering volume. For additional thermostatic shielding the complete setup, with the exception of the light source (He–Ne laser, $\lambda_0 = 632.8 \text{ nm}$, 8mW), was covered by a box with controlled temperature. For reduction of effects from structure-borne sound, the complete experimental arrangement was placed on a vibration-damped optical table. The scattered light was fed to a photomultiplier tube (R647P, Hamamatsu Electronics, Japan) and analyzed using a commercial digital correlator board (ALV-500/E Laser, Langen, Germany), allowing for real-time determination of correlation functions within a characteristic time scale from $2 \times 10^{-7} \text{ s}$ to $3.4 \times 10^3 \text{ s}$.^{65,66} Using a system of slits, lenses, and pinholes, provisions were made to reach a high spatial resolution (scattering volume 10^{-3} mm^3) so that light from only one (spatially) coherent part reached the detector. Accidental fluorescent light was excluded by an interference filter, and contributions from any orientation correlations were avoided by a pair of polarizers.

To check the performance of the light-scattering apparatus a methanol/cyclohexane mixture of critical composition (weight fraction of methanol = 0.2894)⁶⁷ was taken as reference system. Methanol (99.8%, Fluka, Neu-Ulm, Germany) and cyclohexane (99%, Sigma, Steinheim, Germany) were used without additional purification. In Figure 4, the diffusion coefficient D following from our measurements is shown as a function of temperature. Also shown is the graph of the relation

$$D(T) = D_0 t^{\nu^*} \quad (13)$$

with $\nu^* = 0.664^9$ from mode-coupling theory, which is close to the value $\nu^* = 0.671^{68}$ predicted by the dynamic scaling hypothesis. $T_c = 319.56 \pm 0.01 \text{ K}$ and $D_0 = (16.4 \pm 0.2) \times 10^{-10} \text{ m}^2 \text{ s}^{-1}$ follow from a nonlinear regression analysis of our data. The literature value for the critical temperature is $T_c = 319.05 \text{ K}$.⁴¹ Using viscosity data from the literature,^{41,69} relation 9 yields the correlation length of the methanol/cyclohexane mixture as a function of temperature (Figure 5). The $\xi(T)$ data follow the power law behavior of eq 1. If T_c is fixed at the visually determined value, fitting of the theoretical relation eq 1 to the experimental $\xi(T)$ data results in $\xi_0 = 0.32 \pm 0.01 \text{ nm}$, in conformity with values derived from static light-scattering studies, most of which display values in the range $0.32 \text{ nm} \leq \xi_0 \leq 0.39 \text{ nm}$.⁷⁰ We therefore conclude that our

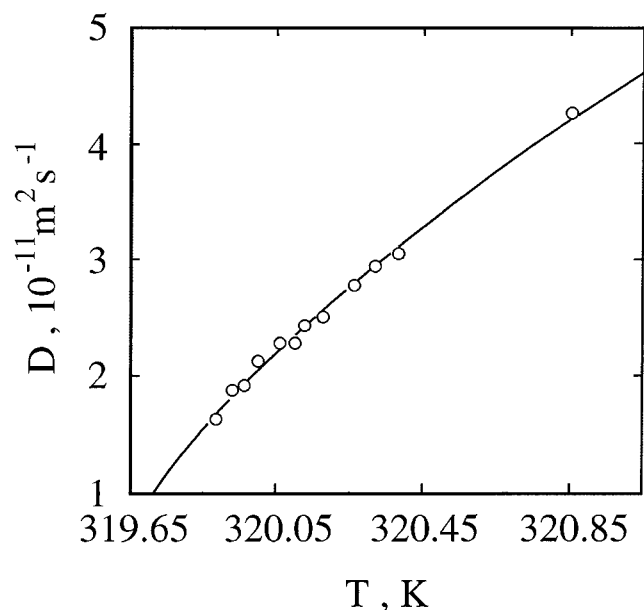


Figure 4. Mutual diffusion coefficient of the methanol/cyclohexane mixture of critical composition plotted versus temperature. The curve is the graph of eq 13 with $\nu^* = 0.664$ and $D_0 = (16.4 \pm 0.2) \times 10^{-10} \text{ m}^2 \text{ s}^{-1}$.

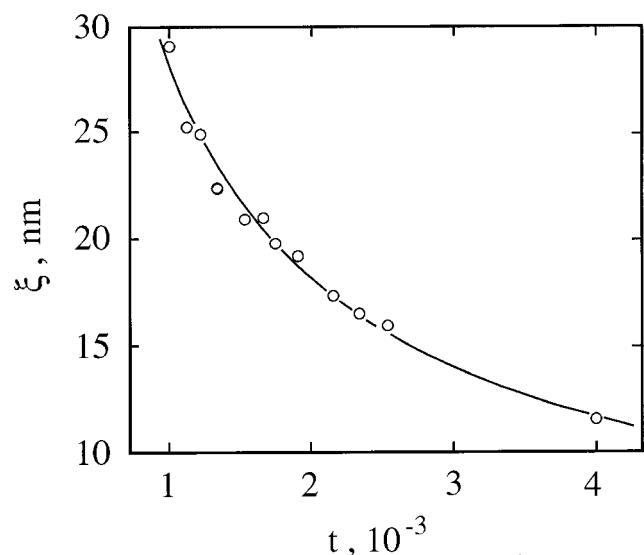


Figure 5. Fluctuation correlation length of the methanol/cyclohexane mixture of critical composition versus reduced temperature t . The curve is the graph of the power law defined by eq 1 with the amplitude $\xi_0 = 3.63 \times 10^{-10} \text{ m}$.

photon correlation spectrometer is well-suited for the dynamic light scattering measurement of the ethanol/dodecane system.

Results and Discussion

Mixture of Critical Composition. In Figure 6, as an example, the ultrasonic excess attenuation spectrum $\alpha_{\lambda \text{exc}}(f, T)$ of the ethanol/dodecane mixture of critical composition is shown at 293.15 K. Here the excess attenuation per wavelength, defined by

$$\alpha_{\lambda \text{exc}}(f, T) = \alpha_{\lambda}(f, T) - \alpha_{\lambda}^b(f, T) \quad (14)$$

has been calculated assuming

$$\alpha_{\lambda}^b(f, T) = B(T)f \quad (15)$$

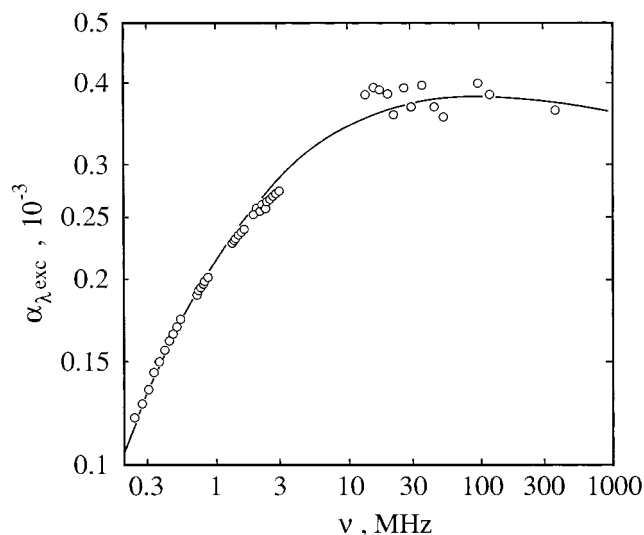


Figure 6. Ultrasonic excess attenuation spectrum of the ethanol/dodecane mixture of critical composition at 20 °C. The curve is the graph of the Bhattacharjee–Ferrell model spectral function $A_{\text{BF}}F_{\text{BF}}(\Omega)$.

with $B(T)$ independent of frequency, in correspondence with the theoretical prediction for the classical contribution² to the total sonic attenuation per wavelength, $\alpha_{\lambda}(f, T)$, and as also appropriate for the consideration of prospective low-frequency wings of high-frequency relaxations with discrete relaxation time. Such a Debye-type contribution ($\omega = 2\pi f$)

$$\alpha_{\lambda D}(f, T) = \frac{A_D \omega \tau_D}{1 + (\omega \tau_D)^2} \approx 2\pi \tau_D A_D f \text{ at } \omega \ll \tau_D^{-1} \quad (16)$$

with relaxation frequency at around 1.3 GHz exists in *n*-dodecane ($A_D = 0.018$, $\tau_D = 0.12 \text{ ns}$, 298.15 K)⁷¹ and has been assigned to the rotational isomerization of the alkane molecules.^{71,72} The example given in Figure 6, where $\alpha_{\lambda \text{exc}} = \alpha_{\lambda}^c$, shows that, even 6.5 K apart from T_c , the excess attenuation spectrum can be well represented by the Bhattacharjee–Ferrell model. Hence the spectral function

$$R_{\text{BF}}(f) = A_{\text{BF}}F_{\text{BF}}(\Omega) + Bf \quad (17)$$

with only three adjustable parameters (A_{BF} , ω_D , B) is sufficient to analytically represent the broadband spectra. At 293.15 K we obtained $A_{\text{BF}} = 1 \times 10^{-3}$, $\omega_D = 5.6 \times 10^6 \text{ s}^{-1}$, $B = 73 \times 10^{-12} \text{ s}$.

In Figure 7 the ω_D values at the eight temperatures closest to T_c are displayed as a function of t . At $t < 2 \times 10^{-2}$ the data follow the power law defined by eq 4, with an amplitude $\omega_0 = (2.8 \pm 0.2) \times 10^9 \text{ s}^{-1}$ and an exponent $z\nu = 1.9 \pm 0.1$. This value for the exponent nicely agrees with the recent accurate value for the viscosity exponent⁵⁷ yielding $z\nu = 1.933 \pm 0.0004$.

At $t > 2 \times 10^{-2}$ ω_D increases stronger than close to the critical temperature. Therefore $\omega_0 = 4.4 \times 10^9 \text{ s}^{-1}$ was found⁴⁹ when all ω_D data up to $t = 9.2 \times 10^{-2}$ had been used (at constant critical exponent) in the regression analysis. Also shown for comparison are the relaxation rates derived from the optically measured diffusion coefficient. These ω_D values have been determined using eq 10 with $\eta(T)$ values as interpolated according to eq 6. The ω_D data, measured at $t < 2 \times 10^{-2}$, also follow a power law eq 4 with $z\nu = 1.94 \pm 0.04$ and $\omega_0 = (8.0 \pm 0.2) \times 10^9 \text{ s}^{-1}$. As mentioned before the theoretical exponent is $z\nu = 1.933$.

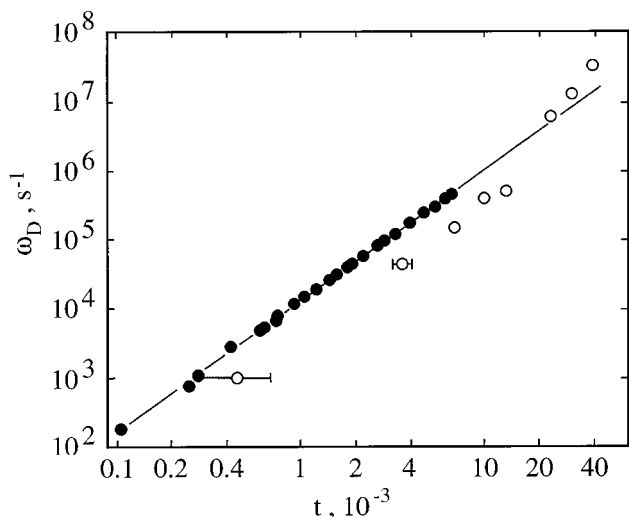


Figure 7. Characteristic relaxation rates as obtained from the light-scattering (●) and the ultrasonic relaxation (○) measurements for the ethanol/dodecane mixture of critical composition shown as a function of reduced temperature. The line represents the power law behavior defined by eq 4.

Bearing in mind the use of rather different methods, the agreement between both sets of relaxation rate data is quite promising (Figure 7). The still-existing difference between the optical and the acoustical data may partly be due to the imperfect temperature control of the specimen cells used in the ultrasonic measurements. It may also partly result from neglect of the noncritical background contributions to the viscosity, diffusion coefficient, and fluctuation correlation length when simple power law behavior is assumed for the total quantities. For the most part, however, the difference seems to reflect the weak dependence of the scaling function upon the reduced frequency (Figure 6). The latter arguments are particularly true for the ethanol/dodecane system for which the critical contributions to the quantities under consideration do not substantially exceed the regular ones.

Let us now more closely inspect the results from the light-scattering measurements. In Figure 8 the fluctuation correlation length ξ is displayed versus the temperature difference $T - T_c$. Each ξ value has been derived from a series of decay rates Γ_q at various scattering angles. Combining eqs 9, 11, and 12

$$\xi_q(T) = \frac{k_B T}{6\pi\eta\Gamma_q} q^2 = \frac{k_B T}{6\pi\eta\Gamma_q} \left(\frac{4\pi n}{\lambda_0}\right)^2 \sin^2\left(\frac{\Theta}{2}\right) \quad (18)$$

follows. Hence fitting this relation to a series of $\xi_q(T, \theta)$ data yields $\xi(T) = \lim_{\Theta \rightarrow 0} \xi_q(T)$. The power law behavior reflected by the ξ -versus- t plot complies with eq 1 with the exponent fixed at the theoretical value $\nu = 0.63^{9,68}$ and with the amplitude $\xi_0 = 0.34 \pm 0.01$ nm.

The plot of Γ_q/q^3 versus $q\xi$ in Figure 9 summarizes the dynamic light-scattering data at different scattering angles. This plot offers a direct method to determine the universal dynamic function $K(q\xi)$ defined by the relaxation rate ω_D of the critical fluctuations and the decay rate Γ_q of the q -dependent order parameter fluctuations⁷³

$$K(q\xi) = 2/(\omega_D\Gamma_q) \quad (19)$$

The universal dynamic function has been first calculated by Kawasaki¹⁰

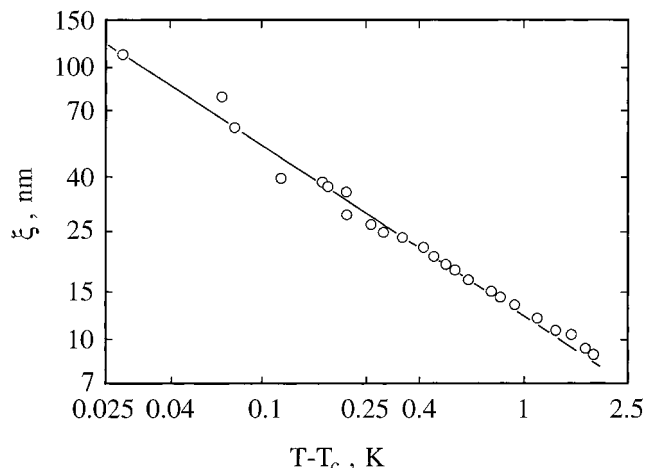


Figure 8. Fluctuation correlation length ξ of the ethanol/dodecane mixture of critical composition displayed versus the distance $T - T_c$ to the critical temperature. The line shows the power law behavior as predicted by eq 1.

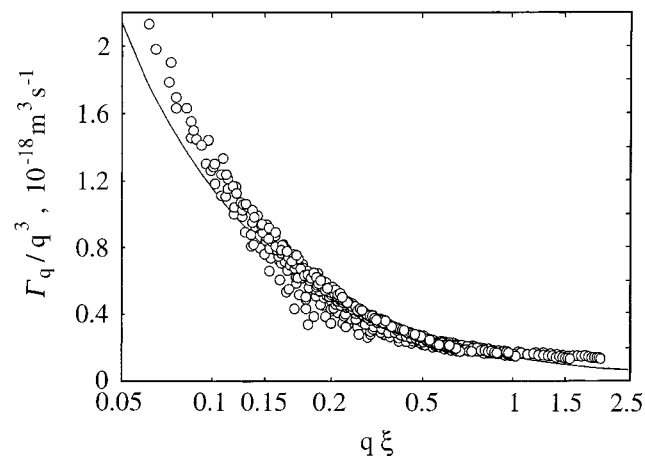


Figure 9. Plot of Γ_q/q^3 versus $q\xi$ for the ethanol/dodecane mixture of critical composition. The curve represents the function $K_0K(q\xi)/(q\xi)$ with an amplitude factor K_0 and the Kawasaki function K as defined by eq 20.

$$K(q\xi) = 3/4(q\xi)^2 \{1 + (q\xi)^2 + [(q\xi)^3 - (q\xi)^{-1}] \arctan(q\xi)\} \quad (20)$$

The curve shown in Figure 9 is the graph of this function. In calculating K the amplitude ω_0 has been treated as an adjustable parameter. We found $\omega_0 = (7.7 \pm 0.7) \times 10^9$ s⁻¹. Even though the agreement between the Kawasaki function $K(q\xi)$ and the measured data is not perfect (Figure 9), the amplitude of the characteristic relaxation rate nicely agrees with the value derived from the light-scattering and the viscosity data ($\omega_0 = 8 \times 10^9$ s⁻¹). Along with $\xi_0 = 0.34$ nm resulting from the correlation length data (Figure 8), the ω_0 value from the fit of the Kawasaki function according to eq 2 yields $D_0 = 4.3 \times 10^{-10}$ m² s⁻¹ for the amplitude of the diffusion coefficient.

Critical Mixtures with Admixed Water. In Figure 10 the mutual diffusion coefficient D is displayed versus temperature T for the mixture of critical composition and for a critical mixture with 0.2%(w/w) water added. The latter sample has been prepared considering also the shift $x' - x$ in the critical mole fraction of ethanol by the presence of admixed water. Here the prime denotes quantities referring to the polluted solution. Following Jacobs and Cohn^{70,74,75} the relation

$$(x'_c - x_c)/x_c = (T'_c - T_c)/T_c \quad (21)$$

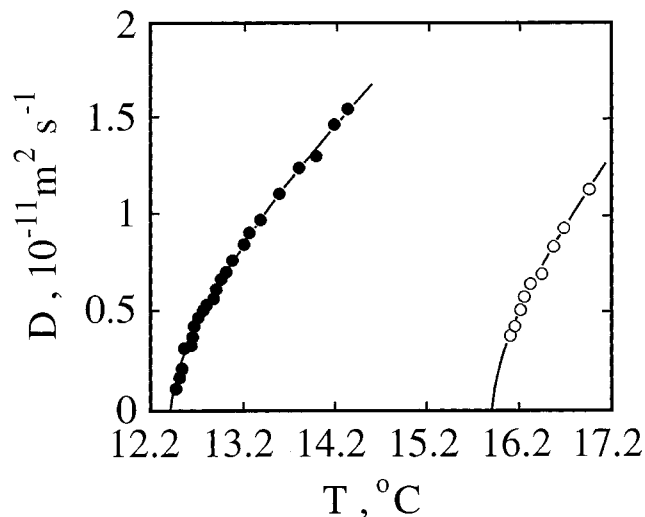


Figure 10. Mutual diffusion coefficient D versus temperature T for the ethanol/dodecane mixture of critical composition without (●) and with water (0.2% w/w, ○) added. The curves indicate the power law behavior defined by eq 13 with T_c adjusted accordingly for the solution with admixed water.

TABLE 1: Parameters of Eq 13 Using the Value $\nu^* = 0.673$ for the Thermal Diffusivity Exponent Displayed for the Ethanol/Dodecane Mixture of Critical Composition without and with Water Added

system	$D_0, 10^{-10} \text{ m}^2 \text{ s}^{-1}$	$T_c, \text{ K}$
pure	4.46 ± 0.05	285.59 ± 0.01
+0.2% (w/w) H_2O	4.91 ± 0.08	289.09 ± 0.01

TABLE 2: Mole Fraction x , Mass Fraction Y , Binodal (T_{bin}) and Pseudospinodal (T_{ps}) Demixing Temperatures as well as Amplitude D_0 of the Mutual Diffusion Coefficient for the Ethanol/Dodecane Mixture of Critical Composition ($x_c = 0.687$) and for Five Mixtures of Noncritical Composition

$x \pm 0.1\%$	$Y \pm 0.05\%$	$T_{\text{bin}}, \text{ K}$ $\pm 0.1 \text{ K}$	$T_{\text{ps}}, \text{ K}$	$D_0, 10^{-10} \text{ m}^2 \text{ s}^{-1}$
0.513	0.2215	284.8	282.26 ± 0.16	6.3 ± 0.2
0.622	0.3082	285.8	285.50 ± 0.01	5.0 ± 0.1
0.687	0.3731	285.6	285.60 ± 0.01	4.5 ± 0.1
0.757	0.4566	285.7	284.66 ± 0.03	5.9 ± 0.1
0.782	0.4928	284.9	283.24 ± 0.06	6.4 ± 0.1
0.823	0.5564	282.5	278.81 ± 4	8.7 ± 1.2

^a The T_{ps} and D_0 data have been obtained from fitting eq 13 to the experimental D -values Using $\nu^* = 0.673$.

holds at small amounts of admixtures. We thus used this relation to calculate the mole fraction $x_c' = 0.3688$ of ethanol for the critical mixture with admixed water.

Applying the power law (eq 13) for the temperature dependence in D to the ethanol/dodecane data displayed in Figure 10, the parameter values given in Table 1 follow. The small amount of admixed water results in a substantial increase in T_c (by about 3.5 K) and it also leads to an enhancement of the amplitude D_0 by about 10%. The D_0 values for the nonpolluted mixture of critical composition are in excellent agreement with the value obtained from a fit of the Kawasaki function (eq 20) to the light-scattering data.

Mixtures of Noncritical Composition. In addition to the mixture of critical composition (mole fraction $x_c = 0.687$ of ethanol) we measured five samples with noncritical composition. The mole fraction and mass fraction of these samples and their binodal demixing temperatures T_{bin} are presented in Table 2. Also given in that table are temperatures T_{ps} following from the pseudospinodal conception.^{51,76} A plot of the T_{bin} and T_{ps}

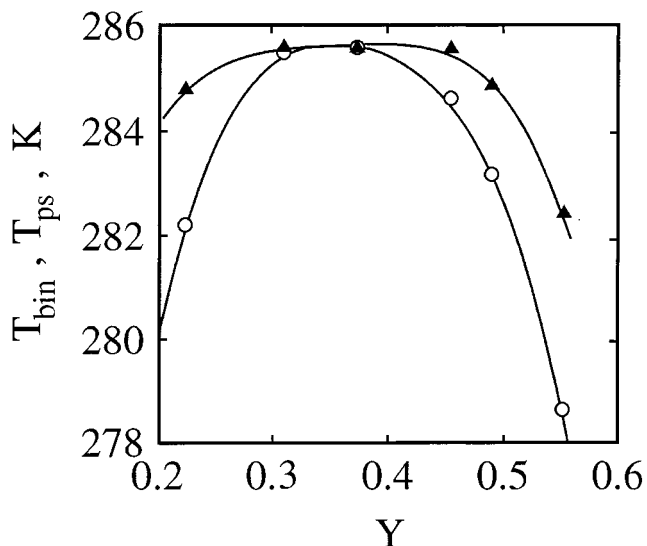


Figure 11. Binodal (T_{bin} , ▲) and the pseudospinodal (T_{ps} , ○) demixing temperatures for the system ethanol/dodecane.

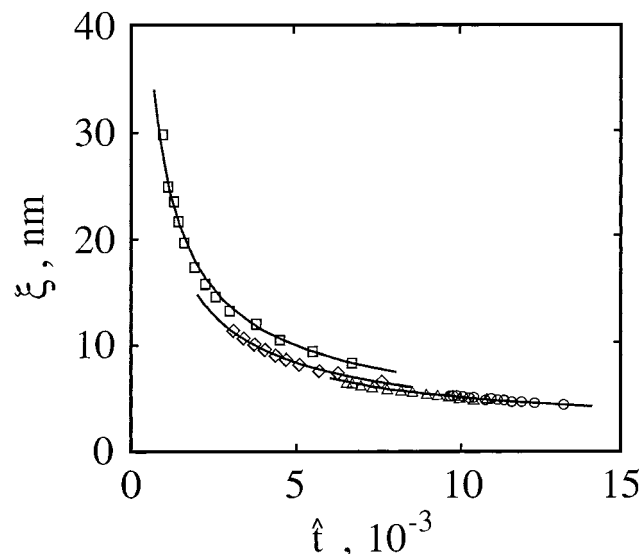


Figure 12. Fluctuation correlation length versus the reduced temperature \hat{t} (eq 22) for four ethanol/dodecane mixtures of noncritical composition (○, $x = 0.513$; △, $x = 0.622$; ◇, $x = 0.757$; □, $x = 0.782$). Curves are drawn to guide the eyes.

data is given in Figure 11. According to the pseudospinodal conception, eq 13 has been analogously applied to the mutual diffusion coefficient data $D(T)$ measured for the mixtures of noncritical composition. In doing so, a reduced temperature \hat{t} that refers to the (hypothetical) temperature T_{ps} instead of a critical temperature may be defined. Hence

$$\hat{t} = |T - T_{\text{ps}}|/T_{\text{ps}} \quad (22)$$

and

$$D(T) = D_0 \hat{t}^{\nu^*} \quad (23)$$

Woermann and co-workers,^{77,78} discussing diffusion coefficient data of binary mixtures, additionally used a noncritical exponent $\hat{\nu}^*$. Our D values have been measured in a too-limited range of reduced temperatures to allow for a decision whether the more general version of the pseudospinodal conception is necessary. Using the power law corresponding to eq 6 to describe the temperature dependence of the viscosities of

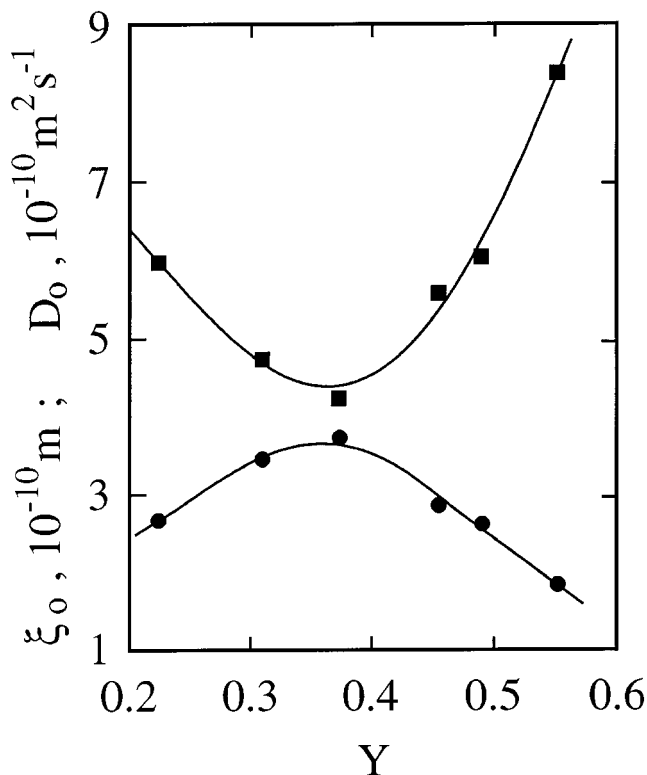


Figure 13. Amplitudes of the correlation length ξ_0 (●) and the diffusion coefficient D_0 (■) of the ethanol/dodecane system as a function of mass fraction Y of ethanol. The curves are drawn to guide the eyes.

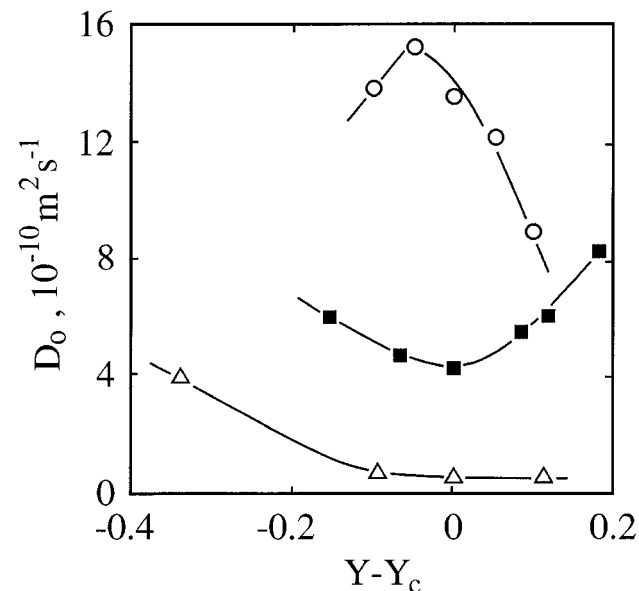


Figure 14. Amplitude of the diffusion coefficient D_0 displayed as a function of mass fraction difference $Y - Y_c$ (Y_c , mass fraction of the mixture of critical composition) for the systems ethanol/dodecane (■), nitrobenzene/isooctane (○),^{40,77} and *n*-amyl alcohol/nitromethane (△).⁸⁰

noncritical mixtures within the framework of the pseudospinodal conception, an almost concentration-independent amplitude $\eta_0 = 1.27 \pm 0.07$ mPa s results. Utilizing the Ferrell–Kawasaki relation (eq 9) the fluctuation correlation lengths of the noncritical mixtures have been calculated from the diffusion coefficients and the viscosities. As shown by the ξ data at four concentrations in Figure 12 the correlation length also follows a power law. In correspondence with eq 1

$$\xi(T) = \xi_0 \hat{t}^{-\hat{\nu}} \quad (24)$$

at $x \neq x_c$. Along with the D_0 data the amplitudes ξ_0 are displayed as a function of mass fraction Y in Figure 13. As to be expected for a system with viscosity amplitude η_0 nearly independent of concentration, the amplitude of the correlation length exhibits a relative maximum at the critical mass fraction Y_c where D_0 adopts a relative minimum. The clear minimum in the D_0 data of the ethanol/dodecane mixtures is different from the results for the systems nitrobenzene/isooctane^{40,77} and *n*-amyl alcohol/nitromethane⁸⁰ reported in the literature (Figure 14). The D_0 values for nitrobenzene/isooctane, which had been obtained using an adjustable exponent $\hat{\nu}^*$ instead of the critical one in eq 24, even show a maximum at Y_c . Also in those former studies, however, a clear-cut conclusion upon the need for a noncritical exponent $\hat{\nu}^* \neq \nu^*$ was not possible. We suppose that a carefully chosen binary system, with properties particularly suited for an optimum scattering behavior, has to be investigated to gain more reliable results on the prospective noncritical exponents $\hat{\nu}^*$.

Acknowledgment. Financial assistance by the DAAD (Bonn, Germany) and the Volkswagen-Stiftung (Hannover, Germany) is gratefully acknowledged.

References and Notes

- (1) Born, M. *Optik*; Springer: Berlin, 1933.
- (2) Herzfeld, K. F.; Litovitz, T. A. *Absorption and Dispersion of Ultrasonic Waves*; Academic Press: New York, 1959.
- (3) Matheson, A. J. *Molecular Acoustics*; Wiley-Interscience: London, 1971.
- (4) Strutt Lord Rayleigh, J. W. *Theory of Sound*, 2nd ed.; Dover: New York, 1945.
- (5) Kaatz, U.; Trachimow, G.; Pottel, R.; Brai, M. *Ann. Phys. (Leipzig)* **1996**, *5*, 13.
- (6) Fixman, M. *J. Chem. Phys.* **1960**, *33*, 1363.
- (7) Fixman, M. *Adv. Chem. Phys.* **1964**, *4*, 175.
- (8) Kawasaki, K. *Phys. Rev.* **1966**, *150*, 291.
- (9) Kawasaki, K. *Ann. Phys.* **1970**, *61*, 1.
- (10) Kawasaki, K. *Phys. Rev. A* **1970**, *1*, 1750.
- (11) Mistura, L. *J. Chem. Phys.* **1972**, *57*, 2311.
- (12) Perl, R.; Ferrell, R. A. *Phys. Rev. A* **1972**, *6*, 2358.
- (13) Chaban, I. A. *Sov. Phys. Acoust.* **1975**, *21*, 177.
- (14) Shiwa, Y.; Kawasaki, K. *Prog. Theor. Phys.* **1981**, *66*, 406.
- (15) Kawasaki, K.; Shiwa, Y. *Physica A* **1982**, *133*, 27.
- (16) Hornowski, T.; Labowski, M. *Acustica* **1990**, *72*, 96.
- (17) Hornowski, T.; Labowski, M. *Arch. Acoust.* **1990**, *15*, 301.
- (18) Bhattacharjee, J. K.; Ferrell, R. A. *Phys. Rev. A* **1981**, *24*, 1643.
- (19) Bhattacharjee, J. K.; Ferrell, R. A. *Phys. Lett.* **1981**, *86A*, 109.
- (20) Ferrell, R. A.; Bhattacharjee, J. K. *Phys. Rev. A* **1985**, *31*, 1788.
- (21) Kadanoff, L. P.; Swift, J. *Phys. Rev.* **1968**, *166*, 89.
- (22) Halperin, B. I.; Hohenberg, P. C. *Phys. Rev.* **1969**, *177*, 952.
- (23) Kroll, D. M.; Ruhland, J. M. *Phys. Lett.* **1980**, *80A*, 45.
- (24) Kroll, D. M.; Ruhland, J. M. *Phys. Rev. A* **1981**, *23*, 371.
- (25) Dengler, R.; Schwabl, F. *Europhys. Lett.* **1993**, *24*, 24.
- (26) Onuki, A. *Phys. Rev. E* **1997**, *55*, 403.
- (27) Onuki, A. *J. Phys. Soc. Jpn.* **1997**, *66*, 511.
- (28) Folk, R.; Moser, G. *Phys. Rev. E* **1998**, *57*, 705.
- (29) Folk, R.; Moser, G. *Phys. Rev. E* **1998**, *58*, 6246.
- (30) Folk, R.; Moser, G. *Int. J. Thermophys.* **1998**, *19*, 1003.
- (31) Tanaka, H.; Wada, Y.; Nakajima, H. *Chem. Phys.* **1982**, *68*, 223.
- (32) Tanaka, H.; Wada, Y.; Nakajima, H. *Chem. Phys.* **1983**, *75*, 37.
- (33) Tanaka, H.; Wada, Y. *Chem. Phys.* **1983**, *78*, 143.
- (34) Garland, C. W.; Sanchez, C. W. *J. Chem. Phys.* **1983**, *79*, 3090.
- (35) Garland, C. W.; Sanchez, C. W. *J. Chem. Phys.* **1983**, *79*, 3100.
- (36) Dunker, H.; Woermann, D.; Bhattacharjee, J. K. *Ber. Bunsen-Ges. Phys. Chem.* **1983**, *87*, 591.
- (37) Jäschke, G.; Dunker, H.; Woermann, D. *Ber. Bunsen-Ges. Phys. Chem.* **1984**, *88*, 630.
- (38) Fast, S. J.; Yun, S. S. *J. Chem. Phys.* **1985**, *83*, 5888.
- (39) Tanaka, H.; Nishi, T.; Wada, Y. *Chem. Phys.* **1985**, *94*, 281.
- (40) Belkoura, L.; Harnisch, F. P.; Kölschens, S.; Müller-Kirschbaum, T.; Woermann, D. *Ber. Bunsen-Ges. Phys. Chem.* **1987**, *91*, 1036.
- (41) Fast, S. J.; Yun, S. S. *J. Acoust. Soc. Am.* **1988**, *83*, 1384.
- (42) Inoue, N.; Murakami, Y.; Kato, M.; Hasegawa, T.; Matsuzawa, K. *Jpn. J. Appl. Phys.* **1992**, *31*, Suppl. 31–1, 66.
- (43) Hornowski, T. *Acta Phys. Pol., A* **1992**, *82*, 961.
- (44) Bittmann, E.; Alig, I.; Woermann, D. *Ber. Bunsen-Ges. Phys. Chem.* **1994**, *98*, 189.

- (45) Zielesny, A.; Woermann, D. *J. Chem. Soc., Faraday Trans.* **1995**, *91*, 3889.
- (46) Hornowski, T.; Labowski, M. *Arch. Acoust.* **1996**, *21*, 53.
- (47) Bhattacharjee, J. K.; Ferrell, R. A. *Physica A* **1998**, *250*, 83.
- (48) Kogan, A. B.; Meyer, H. *J. Low Temp. Phys.* **1998**, *110*, 899.
- (49) Mirzaev, S. Z.; Telgmann, T.; Kaatze, U. *Phys. Rev. E* **2000**, *61*, 542.
- (50) Ferrell, R. A. *Phys. Rev. Lett.* **1970**, *24*, 1169.
- (51) Chu, B.; Schoenes, F. J.; Fisher, M. E. *Phys. Rev.* **1969**, *185*, 219.
- (52) Orzechowski, K. *J. Chem. Soc., Faraday Trans.* **1994**, *90*, 2757.
- (53) Francis, A. W. *Adv. Chem. Ser. N* **1961**, *31*, 77.
- (54) Orzechowski, K. *Physica B* **1991**, *172*, 339.
- (55) Burstyn, H. C.; Sengers, J. V.; Bhattacharjee, J. K.; Ferrell, R. A. *Phys. Rev. A* **1983**, *28*, 1567.
- (56) Berg, R. F.; Moldover, M. R. *J. Chem. Phys.* **1990**, *93*, 1926.
- (57) Berg, R. F.; Moldover, M. R. *Phys. Rev. E* **1999**, *60*, 4079.
- (58) Eggers, F.; Kaatze, U.; Richmann, K. H.; Telgmann, T. *Meas. Sci. Technol.* **1994**, *5*, 1131.
- (59) Kaatze, U.; Wehrmann, B.; Pottel, R. *J. Phys. E: Sci. Instrum.* **1987**, *20*, 1025.
- (60) Kaatze, U.; Lautscham, K.; Brai, M. *J. Phys. E: Sci. Instrum.* **1988**, *21*, 98.
- (61) Fabelenskii, I. L. *Molecular Scattering of Light*; Plenum: New York, 1968.
- (62) *Photon Correlation and Light Beating Spectroscopy*; Cummins, H. Z., Pike, E. R., Eds.; Plenum: New York, 1974.
- (63) Berne, B. J.; Pecora, R. *Dynamic Light Scattering*; Wiley-Interscience: New York, 1976.
- (64) Chu, B. *Laser Light Scattering*; Academic Press: New York, 1991.
- (65) Schätzel, K. *Appl. Phys. B.* **1987**, *42*, 193.
- (66) Schätzel, K.; Drewel, M.; Stimac, M. *Mod. Opt.* **1988**, *35*, 711.
- (67) Jacobs, D. T.; Anthony, D. J.; Mockler R. C.; O'Sullivan, W. J. *Chem. Phys.* **1977**, *20*, 219.
- (68) Hohenberg, P. C.; Halperin, B. I. *Rev. Mod. Phys.* **1977**, *49*, 435.
- (69) Kuskova, N. V.; Matizen, E. V. *JETP Lett.* **1970**, *12*, 174.
- (70) Jacobs, D. T. *J. Chem. Phys.* **1989**, *91*, 560.
- (71) Kaatze, U.; Lautscham, K.; Berger, W. *Chem. Phys. Lett.* **1988**, *144*, 273.
- (72) Behrends, R. Dissertation, Georg-August-Universität: Göttingen, 1999.
- (73) Anisimov M. A. *Critical Phenomena in Liquids and Liquid Crystals*; Gordon and Breach: Philadelphia, 1991.
- (74) Cohn, R. H.; Jacobs, D. T. *J. Chem. Phys.* **1984**, *80*, 856.
- (75) Jacobs, D. T. *Phys. Rev. A* **1986**, *33*, 2605.
- (76) Benedek, G. B. *Polarisation Matière et Rayonnement*; Presses Universitaires de Paris: Paris, 1968.
- (77) Heger, R.; Ikier, C.; Belkoura, L.; Woermann, D. *J. Chem. Soc., Faraday Trans.* **1995**, *91*, 3385.
- (78) Schmitz, J.; Belkoura, L.; Woermann, D. *Ber. Bunsen-Ges. Phys. Chem.* **1995**, *99*, 848.
- (79) Menzel, K. Dissertation, Georg-August-Universität: Göttingen, 1993.
- (80) Labowski, M.; Hornowski, T. *J. Acoust. Soc. Am.* **1987**, *81*, 1421.